Linkages between the cold summer mesopause and thermospheric zonal mean circulation

David E. Siskind,[1] Douglas P. Drob,[1] John T. Emmert,[1] Michael H. Stevens,[1] Patrick E. Sheese,[2] Edward J. Llewellyn,[3] Mark E. Hervig,[4] Rick Niciejewski,[5] and Andrew J. Kochenash[6]

Received 31 October 2011; revised 1 December 2011; accepted 2 December 2011; published 6 January 2012.

[1] We present the first results from the NCAR thermosphere/ionosphere/electrodynamics general circulation model (TIE-GCM) coupled to a weather forecast/assimilation system of the lower and middle atmosphere. Our results emphasize the importance of a proper representation of the latitudinal temperature variation at the base of the thermosphere for calculating zonal mean zonal winds in the thermosphere. The inclusion of a realistic cold summer mesopause yields significantly improved agreement with climatology in the calculated thermospheric winds in the summer hemisphere. Having established this link between the temperature structure of the mesosphere and the thermospheric circulation, we next present observational evidence that the year-to-year variability of thermospheric winds can be linked to analogous variations in the onset of the cold summer mesopause season. Since these mesopause variations have previously been ascribed to stratospheric weather variability, by extension, our results suggest a new mode of coupling between the stratosphere and thermosphere. **Citation:** Siskind, D. E., D. P. Drob, J. T. Emmert, M. H. Stevens, P. E. Sheese, E. J. Llewellyn, M. E. Hervig, R. Niciejewski, and A. J. Kochenash (2012), Linkages between the cold summer mesopause and thermospheric zonal mean circulation, *Geophys. Res. Lett.*, *39*, L01804, doi:10.1029/2011GL050196.

1. Introduction

[2] It is now established that significant perturbations to the thermosphere and ionosphere can result from meteorological disturbances that originate in the lower atmosphere. In an effort to understand this variability, a new generation of models now encompasses both the lower and upper atmosphere. These models are often termed "seamless", because they have a single dynamical solver that simulates the approximately 12 orders of atmospheric density from the surface to the exobase [see *Akmaev*, 2011, and references therein].

[3] Here we present initial results using by coupling two models together. While we give up the advantage of seamlessness, we acquire, as we will discuss, the ability to specify better meteorological conditions for a given date and time. Our primary thermosphere model is the NCAR TIE-GCM [*Richmond et al.*, 1992]. In this paper, we introduce a new way to specify the lower boundary of the TIE-GCM by using the NOGAPS-ALPHA forecast/assimilation system [*Eckermann et al.*, 2009]. As discussed by *Ren et al.* [2011], the use of a mesospheric analysis can offer some advantages in that it relaxes some of the requirements on a gravity wave drag parameterization while still insuring that the larger spatial scales are simulated accurately. We examine the zonal mean zonal wind in the lower thermosphere and demonstrate improved agreement with the Horizontal Wind Model (HWM07) [*Drob et al.*, 2008].

[4] In addition, after establishing the link between thermospheric zonal winds and the middle atmosphere temperature structure, we will present observational evidence suggesting that interannual variability in thermospheric zonal winds can be linked to similar variability in the mesopause. Several recent papers have linked variations in stratospheric weather phenomena to the seasonal development of the cold summer mesopause through gravity wave modulation by the variable zonal wind. *Smith et al.* [2010] linked long term trends associated with the growth of the ozone hole with the cold mesopause. *Karlsson et al.* [2011] and *Gumbel and Karlsson* [2011] emphasized the dramatic year-to-year variability in the onset of polar mesospheric clouds (PMCs) in the Southern Hemisphere (SH) as recorded by the NASA Aeronomy of Ice in the Mesosphere (AIM) satellite. Our results offer observational support for these published model predictions. We analyze data from three instruments: temperatures from the Solar Occultation for Ice Experiment (SOFIE) on AIM [*Gordley et al.*, 2009], and from the Optical Spectrograph and Infrared Imaging System (OSIRIS) [*Sheese et al.*, 2011], and winds from the TIMED Doppler Interferometer (TIDI) [*Niciejewski et al.*, 2006]. Further, by showing that this interannual variability extends well into the thermosphere, our results suggest a new coupling mechanism between the stratosphere and the thermosphere, and possibly the ionosphere.

2. Modeling Approach

[5] The TIE-GCM is a first-principles thermosphere-ionosphere general circulation model that extends from about 95 km to the upper thermosphere and includes a specific calculation of tropical induced electric fields and resultant ion drifts from ion-neutral coupling in the lower

[1]Space Science Division, Naval Research Laboratory, Washington, D. C., USA.
[2]Department of Atmospheric Physics, University of Toronto, Toronto, Ontario, Canada.
[3]Department of Physics and Engineering Physics, University of Saskatchewan, Saskatoon, Saskatchewan, Canada.
[4]GATS Inc., Driggs, Idaho, USA.
[5]Space Physics Research Laboratory, University of Michigan, Ann Arbor, Michigan, USA.
[6]Computational Physics Inc., Springfield, Virginia, USA.

0094-8276/12/2011GL050196

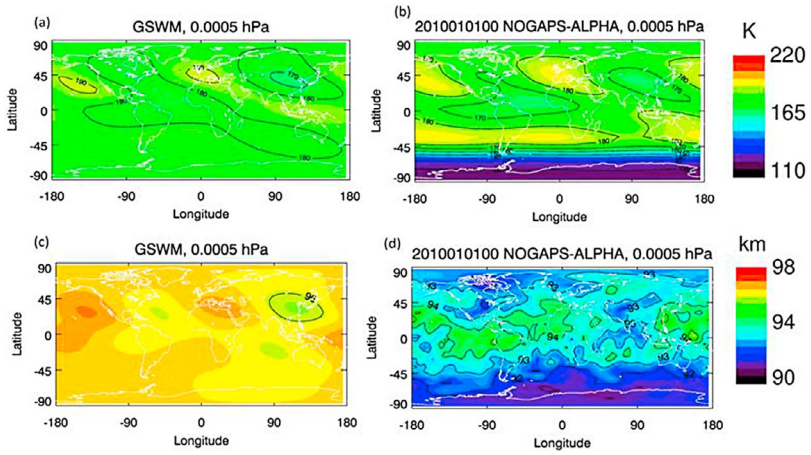

Figure 1. Temperature and geopotential height distributions as a function of latitude and longitude for two different bottom boundary conditions for the TIE-GCM, (a) temperature perturbation from the GSWM model for December solstice, solar minimum conditions with a fixed global average temperature of 181 K, (b) temperature from the NOGAPS-ALPHA forecast model for January 1, 2010, 00UT with a global average 10 K bias correction added (see text), (c) geopotential heights associated with Figure 1a, (d) geopotential heights associated with Figure 1b.

thermosphere. *Fesen et al.* [2000] showed that a realistic diurnal variation of the equatorial ion drift could be achieved, including the enhancement of the vertical drift prior to its evening reversal. The TIE-GCM allows for the specification of varying solar EUV irradiance and geomagnetic inputs such as particle precipitation and convection electric fields. Since the simulations shown here are for a period during the recent solar minimum, we used fixed and low values for solar-terrestrial forcing (Solar $F_{10.7}$ index = 70 sfu, auroral hemispheric power = 8 GW, and the cross polar cap electric potential drop = 30 kV).

[6] We are specifically interested in the bottom boundary of the TIE-GCM, which is at a level z = −7, where $z = -\ln(P_o/P)$ and P_o is 5×10^{-7} mb. In the standard configuration, (http://www.hao.ucar.edu/modeling/tgcm/doc/description/model_description.pdf; we used V1.93 for this work), the bottom boundary includes migrating diurnal and semidiurnal tides as specified by the Global Scale Wind Model (GSWM) [*Hagan et al.*, 2001] together with a fixed, globally averaged (i.e., independent of day of year, latitude, and longitude) background temperature of 181 K and zero background winds. This configuration has been used in the most recent implementations of TIE-GCM [e.g., *Kondo et al.*, 2011; *Solomon et al.*, 2011]. Here, we instead use output from the Navy Operational Global Atmospheric Prediction System- Advanced Level Physics High Altitude (NOGAPS-ALPHA) forecast/assimilation model to provide temperatures, geopotential heights, and zonal and meridional winds [*Eckermann et al.*, 2009]. The NOGAPS-ALPHA analysis uses the NRL Atmospheric Variational Data Assimilation system (NAVDAS). One limitation of NAVDAS is that its 6 hourly update cycle might lead to aliasing of semi-diurnal and higher-order tidal modes. Also, the bottom boundary of the TIE-GCM corresponds almost identically to the top pressure of the NOGAPS-ALPHA analysis. This is a problem because the top two pressure levels of the analysis are used as a sponge layer. In contrast, the forecast model component of NOGAPS-ALPHA, which can be initialized from the analysis, can be configured to provide 1 hourly output and extends a decade in pressure higher in altitude than the analysis. For the results shown here, we used this 1 hourly product, re-initialized every 6 hours, for the first 30 days of January 2010. The resultant 720 hourly outputs were used as a bottom boundary of the TIE-GCM.

[7] Figure 1 compares the temperatures and associated geopotential heights for two possible bottom boundary conditions for the TIE-GCM. Figure 1a shows a GSWM temperature field for December solstice, solar minimum conditions. The wave-two pattern of the semidiurnal tide is clearly apparent in the winter hemisphere. Figure 1b shows a sample output temperature field at 0.0005 hPa from NOGAPS-ALPHA (initialized by NAVDAS) for January 1st, 2010, 00UT. NOGAPS-ALPHA also shows a wave-two tidal pattern in the winter hemisphere; however, it additionally shows the sharp latitudinal temperature gradient in the summer hemisphere, where temperatures fall below 130 K for this specific time. This reflects the effects of the summer mesopause, which is at about 88–90 km, just several km lower than the mean altitude associated with the 0.0005 hPa surface. Figure 1c shows the near constant

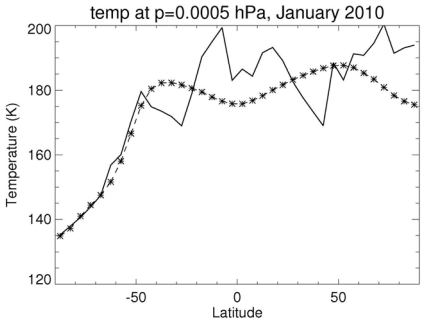

Figure 2. Zonal mean temperature for the bottom boundary of the TIE-GCM. The stars are from the 720 hourly outputs of NOGAPS-ALPHA. A latitudinally invariant 10 K cold bias was corrected for. The solid line is monthly averaged data from OSIRIS for January 2010.

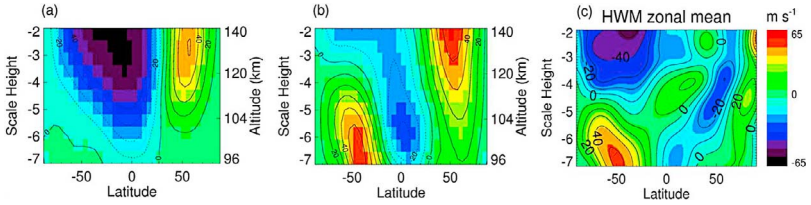

Figure 3. Monthly mean zonal winds from the TIE-GCM for (a) a bottom boundary with migrating tides and globally invariant temperature and (b) the NOGAPS-ALPHA bottom boundary as summarized in Figure 1. (c) Monthly mean climatology from the HWM07 climatology [*Drob et al.*, 2008].

geopotential height distribution associated with the GSWM temperature field. Figure 1d shows the geopotential heights associated with the NOGAPS-ALPHA field. The pronounced decrease in the heights towards the summer pole is evident. This decrease, of about 3 km (from 94 to 91 km), is typical of what is associated with the wintertime stratospheric polar vortex [cf. *Andrews et al.*, 1987, Figure 5.6].

[8] To validate our bottom boundary, we compared an average of zonal mean temperatures for January 2010 from OSIRIS [*Sheese et al.*, 2011] with the corresponding average of the hourly forecast product. The results, given in Figure 2, show excellent agreement, especially in the summer hemisphere. In absolute value, the forecast model was colder than OSIRIS, and thus Figures 1b and 2 have a 10 K latitudinally invariant correction applied to the model; this bias correction had no impact on our calculated thermospheric winds, because it is the latitudinal *gradient* that is balanced by the zonal flow, according to the thermal wind relation.

3. Modeling Results

[9] Figure 3 compares the monthly average zonal mean zonal wind for the lower thermosphere from the two configurations of the TIE-GCM. The left and center panels show results using the lower boundary conditions summarized in Figures 1a (GSWM) and 1b (NOGAPS-ALPHA), respectively. The TIE-GCM was first "spun-up" for 30 days with fixed inputs in order to ensure that the winds and temperatures were balanced. The resulting winds differ strikingly between the two solutions, particularly in the summer hemisphere. The right panel shows the climatology of zonal winds from the HWM07 model. It is apparent that the NOGAPS-forced model yields a dramatically improved agreement with the climatology, most notably in a strong summertime lower thermospheric eastward jet. This jet is the simple result of thermal wind balance above the cold summer mesopause and demonstrates the importance of an accurate representation of mesospheric temperatures. Indeed, the difference between the NOGAPS-forced and the GSWM-forced solution covers the entire domain that we present and extends into the tropics, where ion-neutral coupling is known to be important [*Liu et al.*, 2010]. It is therefore plausible to suggest that ionospheric calculations should also take into account mesospheric temperature structures.

4. Observed Interannual Variability in Temperatures and Winds

[10] Having established the importance of a proper representation of the cold summer mesopause on simulations of thermosphere circulation, we now consider interannual variability in the mesopause and possible connections to the thermosphere. *Gumbel and Karlsson* [2011] have shown that two recent years differed dramatically in the onset of the cold SH summer season. In 2009 the season occurred early, with PMCs detected by mid-November. In 2010 the season occurred unusually late, with PMCs not detected until mid-December. Gumbel and Karlsson suggest that the difference resulted from changes in the timing of the breakdown in the stratospheric polar vortex, which is associated with the Antarctic ozone hole. The polar vortex blocks the gravity waves which, upon breaking, cause the cold summer mesopause. Unfortunately, the NOGAPS-ALPHA analysis does not extend past March 2010 so we can not yet simulate this period. However, *Karlsson et al.* [2011] provided some model predictions for early and late seasonal onsets. Here we present some observational data that we compare with their predictions.

[11] Figure 4 shows averaged temperature profiles for the onset period of the cold SH summer mesopause (late November to mid-December). The SOFIE data extend from the stratosphere up to 90–95 km and the OSIRIS data extend from 88 to 105 km. It is apparent that in the region of overlap, OSIRIS is colder than SOFIE; this is well known and is currently being quantified by us in a SOFIE validation paper (M. H. Stevens et al., manuscript in preparation, 2011). Here, however, we are only interested in the difference between 2009 and 2010 and this is the same for both datasets. In the onset period for the early vortex breakdown year (2009), the mesopause region was colder than during the onset period for the year of late vortex breakdown (2010). Interestingly, above the mesopause both SOFIE and OSIRIS indicate a change in sign in the temperature difference between 2009 and 2010. Between 95 and 100 km,

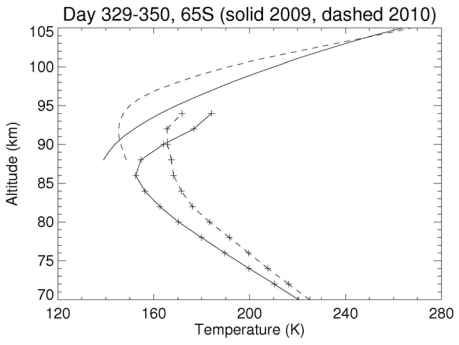

Figure 4. Temperatures, averaged over days 329–350 in 2009 (solid) and 2010 (dashed), from SOFIE (lower curves with symbols) and OSIRIS (upper curves). The OSIRIS data are a latitudinal average from 60°S to 70°S.

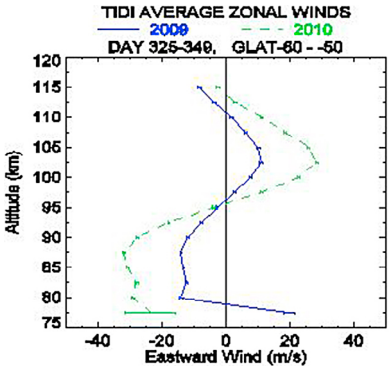

Figure 5. Averaged zonal winds for 50°S–60°S during days 325–349 of 2009 (blue solid) and 2010 (green dashed) from TIDI. All local times are nonuniformly sampled by this bin. The local time sampling is the same for 2009 and 2010. Error bars denote the standard error of the mean as deduced from the instrumental uncertainty.

OSIRIS measured temperatures that are 20 K colder in 2010 (the late breakdown year). This is in good agreement with Figure 6b of *Karlsson et al.* [2011], who ascribe it to a change in the breaking level of the eastward propagating gravity waves.

[12] From thermal wind considerations, and bolstered by our model results in Figure 3, we expect these temperature anomalies to be balanced by concomitant zonal wind changes extending into the thermosphere. Figure 5 presents data from TIDI that shows this is indeed the case. In general, the colder polar temperatures are balanced by greater eastward flow at higher altitudes (recall that thermal wind balance actually refers to the vertical gradient of the zonal wind). Note that TIDI does not give a true zonal mean since it does not sample all local times evenly during the period considered; however, since the local time sampling repeats from year to year, the interannual comparison is robust. Below 90 km, since 2009 is colder, we see greater eastward flow (or equivalently, reduced westward flow in this case). This agrees with Figure 6a of *Karlsson et al.* [2011]. However, above 95 km, since 2010 is colder at these altitudes, we see greater eastward flow in this year. TIDI shows that this interannual variability extends up to 115 km, the top of its observable range. This is 15 km above the altitudes presented by *Karlsson et al.* [2011], but is generally consistent with our TIE-GCM results, which also show effects of mesopause temperatures persisting well up into the thermosphere.

5. Discussion

[13] The combination of our coupled NOGAPS-ALPHA/TIE-GCM results and the observed changes in temperatures and zonal wind in 2009 and 2010 show that mesopause temperature variability can influence altitudes well into the thermosphere, at least up to 115 km. Since ion-neutral coupling begins to be important above 100 km, we speculate that these changes could influence ionospheric structure. Since, in turn, mesopause temperature variability has been linked to changes in the stratospheric polar vortex, itself linked to trends in the Antarctic ozone hole, the combination of our results with *Karlsson et al.* [2011] and *Smith et al.* [2010] suggests a new mode of coupling between the stratosphere and the thermosphere and possibly the ionosphere. Studies of interannual ionospheric variability should consider interannual variability and trends in the depth and duration of the Antarctic ozone hole, in order to see if this connection is robust.

[14] **Acknowledgments.** This work was funded by the Office of Naval Research and the NASA Aeronomy of Ice in the Mesosphere (AIM) project. We thank the National Center for Atmospheric Research for the use of the TIE-GCM.

[15] The Editor thanks the two anonymous reviewers for their assistance in evaluating this paper.

References

Akmaev, R. A. (2011), Whole atmosphere modeling: Connecting terrestrial and space weather, *Rev. Geophys.*, *49*, RG4004, doi:10.1029/2011RG000364.

Andrews, D. G., J. R. Holton, and C. B. Leovy (1987), *Middle Atmospheric Dynamics*, 489 pp., Academic, Orlando, Fla.

Drob, D. P., et al. (2008), An empirical model of the Earth's horizontal wind fields: HWM07, *J. Geophys. Res.*, *113*, A12304, doi:10.1029/2008JA013668.

Eckermann, S. D., et al. (2009), High altitude data assimilation system experiments for the Northern Hemisphere summer mesosphere season of 2007, *J. Atmos. Sol. Terr. Phys.*, *71*, 531–551, doi:10.1016/j.jastp.2008.09.036.

Fesen, C. G., G. Crowley, R. G. Roble, A. D. Richmond, and B. G. Fejer (2000), Simulation of the pre-reversal enhancement in the low latitude vertical ion drifts, *Geophys. Res. Lett.*, *27*, 1851–1854, doi:10.1029/2000GL000061.

Gordley, L. L., et al. (2009), The solar occultation for ice experiment, *J. Atmos. Sol. Terr. Phys.*, *71*, 300–315, doi:10.1016/j.jastp.2008.07.012.

Gumbel, J., and B. Karlsson (2011), Intra- and inter-hemispheric coupling effects on the polar summer mesosphere, *Geophys. Res. Lett.*, *38*, L14804, doi:10.1029/2011GL047968.

Hagan, M. E., R. G. Roble, and J. Hackney (2001), Migrating thermospheric tides, *J. Geophys. Res.*, *106*, 12,739–12,752, doi:10.1029/2000JA000344.

Karlsson, B., C. E. Randall, T. G. Shepherd, V. L. Harvey, J. Lumpe, K. Nielsen, S. M. Bailey, M. Hervig, and J. M. Russell III (2011), On the seasonal onset of polar mesospheric clouds and the breakdown of the stratospheric polar vortex in the Southern Hemisphere, *J. Geophys. Res.*, *116*, D18107, doi:10.1029/2011JD015989.

Kondo, T., A. D. Richmond, H. Liu, J. Lei, and S. Watanabe (2011), On the formation of a fast thermospheric zonal wind at the magnetic dip equator, *Geophys. Res. Lett.*, *38*, L10101, doi:10.1029/2011GL047255.

Liu, H.-L., W. Wang, A. D. Richmond, and R. G. Roble (2010), Ionospheric variability due to planetary waves and tides for solar minimum conditions, *J. Geophys. Res.*, *115*, A00G01, doi:10.1029/2009JA015188.

Niciejewski, R., Q. Wu, W. Skinner, D. Gell, M. Cooper, A. Marshall, T. Killeen, S. Solomon, and D. Ortland (2006), TIMED Doppler Interferometer on the Thermosphere Ionosphere Mesosphere Energetics and Dynamics satellite: Data product overview, *J. Geophys. Res.*, *111*, A11S90, doi:10.1029/2005JA011513.

Ren, S., S. Polavarapu, S. R. Beagley, Y. Nezlin, and Y. J. Rochon (2011), The impact of gravity wave drag on mesospheric analyses of the 2006 stratospheric major warming, *J. Geophys. Res.*, *116*, D19116, doi:10.1029/2011JD015943.

Richmond, A. D., E. C. Ridley, and R. G. Roble (1992), A thermosphere-ionosphere general circulation model with coupled electrodynamics, *Geophys. Res. Lett.*, *19*, 601–604, doi:10.1029/92GL00401.

Sheese, P. E., E. J. Llewellyn, R. L. Gattinger, A. E. Bourassa, D. A. Degenstein, N. D. Lloyd, and I. C. McDade (2011), Mesopause temperatures during the polar mesospheric cloud season, *Geophys. Res. Lett.*, *38*, L11803, doi:10.1029/2011GL047437.

Smith, A. K., R. R. Garcia, D. R. Marsh, D. E. Kinnison, and J. H. Richter (2010), Simulations of the response of mesospheric circulation and temperature to the Antarctic ozone hole, *Geophys. Res. Lett.*, *37*, L22803, doi:10.1029/2010GL045255.

Solomon, S. C., L. Qian, L. V. Didkovsky, R. A. Viereck, and T. N. Woods (2011), Causes of low thermospheric density during the 2007–2009 solar minimum, *J. Geophys. Res.*, *116*, A00H07, doi:10.1029/2011JA016508.

D. P. Drob, J. T. Emmert, D. E. Siskind, and M. H. Stevens, Space Science Division, Naval Research Laboratory, 4555 Overlook Ave. SW, Washington, DC 20375, USA. (david.siskind@nrl.navy.mil)

M. E. Hervig, GATS Inc., PO Box 449, Driggs, ID 83422, USA.

A. J. Kochenash, Computational Physics Inc., 8001 Braddock Rd., Ste. 210, Springfield, VA 22151, USA.

E. J. Llewellyn, Department of Physics and Engineering Physics, University of Saskatchewan, 116 Science Pl., Saskatoon, SK S7N 5E2, Canada.

R. Niciejewski, Space Physics Research Laboratory, University of Michigan, 2455 Hayward St., Ann Arbor, MI 48109, USA.

P. E. Sheese, Department of Atmospheric Physics, University of Toronto, 60 St. George St., Toronto, ON M5S 1A7, Canada.